*Article*

**aeroacoustics**

*International Journal of Aeroacoustics*
2019, Vol. 18(1) 92–111

DOI: 10.1177/1475472X18812802
journals.sagepub.com/home/jae
SAGE

# Radiation analysis of sound waves from semi-infinite coated pipe

**Burhan Tiryakioglu[1] and Ahmet Demir[2]**

**Abstract**

An analytical solution is presented for the problem of radiation of sound waves from a semi-infinite circular cylindrical coated pipe which is partially lined from inside. By stating the total field in duct region in terms of normal waveguide modes (Dini's series) and using the Fourier transform technique elsewhere, we obtain a Wiener–Hopf equation whose solution involving three sets of infinitely many unknown expansion coefficients satisfying three systems of linear algebraic equations. This system is solved numerically and the influence of some parameters (pipe radius, impedances, extension, etc.) on the radiation phenomenon is displayed graphically.

**Keywords**

Wiener–Hopf, acoustic, sound radiation, mode matching, pipe

Date received: 9 January 2018; accepted: 2 July 2018

## Introduction

Today, the world's population is 7.3 billion people and it continues to grow; hence, the number of cars and aircraft is increasing day by day. Since, the highways and airports are built nearby the city centers, this situation, especially for the people who living in urban area, leads to the formation of excessive noise. Accordingly, reduction of noise pollution has become very important in order to improve the quality of life.[1–4]

Researchers, who want to reduce noise pollution, investigated the sound radiation, and some effective methods were found.[5–10] For example, the propagation of sound in

[1]Department of Applied Mathematics, Marmara University, İstanbul, Turkey
[2]Department of Mechatronics Engineering, Karabuk University, Karabuk, Turkey

**Corresponding author:**
Burhan Tiryakioglu, Department of Applied Mathematics, Marmara University, Istanbul, 34722, Turkey.
Email: burhan.tiryakioglu@marmara.edu.tr

cylindrical ducts or pipes which can be assumed as a model of car exhaust or aircraft engine etc. Absorbent lining is an effective method of reducing noise from pipes.[11–14]

Rawlins considered the radiation of sound from a rigid cylindrical duct with an acoustically absorbing internal surface.[15] The lining is modelled by an impedance boundary condition. An analytical solution is obtained based on the Wiener–Hopf technique[16] which was proven to be a very important method in engineering and mathematical physics. Demir and Buyukaksoy then treated a similar problem now with a partial lining.[17] A hybrid formulation which consists of employing the Fourier transform technique in conjunction with the Mode Matching method was applied successfully for the solution. In both studies above, some numerical results were also given graphically.

The goal of the present work is to study the radiation of sound waves by a semi-infinite lined pipe where a part of its interior surface is treated with an acoustically absorbing material. The method adopted here is similar to that employed in Demir and Buyukaksoy[17] and consists of expressing the total field in the waveguide region in terms of normal waveguide modes and using the Fourier Transform elsewhere. Then, the related boundary-value problem is formulated as a modified Wiener–Hopf equation of the second kind whose solution involve a set of infinitely many expansion coefficients satisfying an infinite system of linear algebraic equations. Numerical solution of this system is obtained for various values of the parameters of the problem such as pipe radius ($a$), internal and external surface impedances ($\eta, \beta$), hard outer ($\beta \to 0$), hard inner ($\eta \to 0$) and hard pipe ($\beta, \eta \to 0$) – lined pipe cases, pipe extension ($l$), reflection coefficient ($c_0$) and comparison with previous work,[17] and their effects on the radiation phenomenon are shown graphically.

The time dependence is assumed to be $exp(-i\omega t)$, with $\omega$ being the angular frequency, and is suppressed throughout the paper.

## Analysis

### *Formulation of the problem*

Consider the radiation of sound waves by a semi-infinite circular cylindrical pipe defined by $\{\rho = a, \phi \in (-\pi, \pi), z \in (-\infty, l)\}$ (see Figure 1) where $(\rho, \phi, z)$ denote the usual cylindrical coordinates. The outer part is lined with an acoustically absorbent material having a surface impedance $\beta$, while the inner part is coated by another acoustically absorbent material which is characterized by a surface impedance $\eta$. From the symmetry of the geometry of

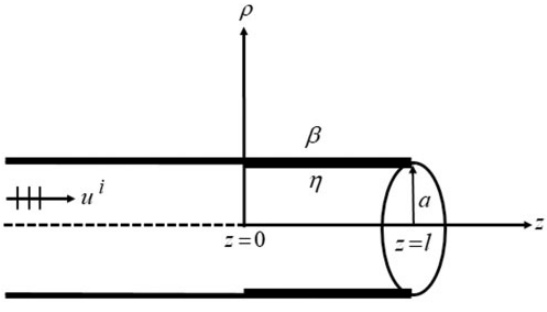


**Figure 1.** Geometry of the problem.

the problem and of the incident field, the acoustic field will be independent of $\phi$ everywhere. We shall therefore introduce a scalar potential $u(\rho, z)$ which defines the acoustic pressure and velocity by $p = i\omega\rho_0 u$ and $\mathbf{v} = \text{grad}u$, respectively, where $\rho_0$ is the density of undisturbed medium.

The incident sound wave which is propagating in the rigid pipe is taken to be

$$u^i = e^{ikz} \tag{1}$$

where $k = \omega/c$ denotes the wave number of the space and $c$ is the speed of sound. An expression of the total field will be established as follows

$$u^T = \begin{cases} u_1(\rho, z); & \rho > a, \quad z \in (-\infty, \infty) \\ u_2(\rho, z); & \rho < a, \quad z > l \\ u_3(\rho, z); & \rho < a, \quad 0 < z < l \\ u_4(\rho, z) + u^i; & \rho < a, \quad z < 0 \end{cases} \tag{2}$$

$u_j$, $j = 1 - 4$, which satisfy the Helmholtz equation, are to be determined with the aid of the following boundary and continuity relations.

The boundary condition on the absorbent surface can be given in terms of the potential functions $u_1$ and $u_3$

$$\left(ik\beta + \frac{\partial}{\partial\rho}\right)u_1(a, z) = 0, \quad z < l \tag{3a}$$

$$\left(ik\eta - \frac{\partial}{\partial\rho}\right)u_3(a, z) = 0, \quad z < l \tag{3b}$$

The inner pipe wall is rigid for $z < 0$, so that

$$\frac{\partial}{\partial\rho}u_4(a, z) = 0, \quad z < 0 \tag{3c}$$

Consider now the continuity conditions related to total field at $\rho = a, z > l$ which are given by

$$\frac{\partial}{\partial\rho}u_1(a, z) - \frac{\partial}{\partial\rho}u_2(a, z) = 0, \quad z > l \tag{3d}$$

$$u_1(a, z) - u_2(a, z) = 0, \quad z > l \tag{3e}$$

From the continuity at the point $z = l$ and $z = 0$, we get

$$\frac{\partial}{\partial z}u_2(\rho, l) - \frac{\partial}{\partial z}u_3(\rho, l) = 0, \quad \rho < a \tag{3f}$$

$$u_2(\rho, l) - u_3(\rho, l) = 0, \quad \rho < a \tag{3g}$$

$$\frac{\partial}{\partial z} u_3(\rho, 0) - \frac{\partial}{\partial z} u_4(\rho, 0) = ik, \quad \rho < a \tag{3h}$$

$$u_3(\rho, 0) - u_4(\rho, 0) = 1, \quad \rho < a \tag{3i}$$

## Modified Wiener–Hopf equation

The unknown fields $u_j$, $j = 1 - 4$ satisfy the Helmholtz equation for $z \in (-\infty, \infty)$

$$\left[\frac{1}{\rho}\frac{\partial}{\partial \rho}\left(\rho \frac{\partial}{\partial \rho}\right) + \frac{\partial^2}{\partial z^2} + k^2\right] u_j(\rho, z) = 0, \quad \text{j} = 1 - 4 \tag{4}$$

Since $u_1(\rho, z)$ satisfies the Helmholtz equation in the range $z \in (-\infty, \infty)$, its Fourier transform with respect to $z$ gives

$$\left[\frac{1}{\rho}\frac{\partial}{\partial \rho}\left(\rho \frac{\partial}{\partial \rho}\right) + (k^2 - \alpha^2)\right] F(\rho, \alpha) = 0 \tag{5}$$

with

$$F(\rho, \alpha) = \int_{-\infty}^{\infty} u_1(\rho, z) e^{i\alpha z} \mathrm{d}z = e^{i\alpha l}\left(F^{-}(\rho, \alpha) + F^{+}(\rho, \alpha)\right) \tag{6}$$

where

$$F^{-}(\rho, \alpha) = \int_{-\infty}^{l} u_1(\rho, z) e^{i\alpha(z-l)} \mathrm{d}z \tag{7a}$$

$$F^{+}(\rho, \alpha) = \int_{l}^{\infty} u_1(\rho, z) e^{i\alpha(z-l)} \mathrm{d}z \tag{7b}$$

It can be seen that $F^{+}(\rho, \alpha)$ and $F^{-}(\rho, \alpha)$ are analytic functions of $\alpha$ in the half-planes $\Im m\alpha > \Im m(-k)$ and $\Im m\alpha < \Im mk$, respectively. The solution of equation (5) reads

$$e^{i\alpha l}\left(F^{-}(\rho, \alpha) + F^{+}(\rho, \alpha)\right) = A(\alpha) H_0^{(1)}(K\rho) \tag{8}$$

with

$$K(\alpha) = \sqrt{k^2 - \alpha^2} \tag{9}$$

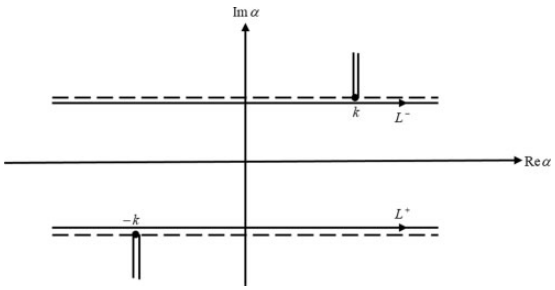


**Figure 2.** Branch cuts in the complex plane.

where $A(\alpha)$ is a spectral coefficient to be determined. The square-root function $K(\alpha)$ is defined in the complex $\alpha-$plane cut as shown in Figure 2 such that $K(0) = k$.

Consider now the Fourier transform of (3a), namely

$$e^{i\alpha l}\left(ik\beta F^{-}(a,\alpha) + \dot{F}^{-}(a,\alpha)\right) = 0 \tag{10}$$

where the dot specifies the derivative with respect to $\rho$. By taking the derivative of equation (8) with respect to $\rho$ and then using equation (10), we obtain, after putting $\rho = a$

$$e^{i\alpha l}W^{+}(\alpha) = A(\alpha)H(\alpha) \tag{11}$$

where

$$W^{+}(\alpha) = ik\beta F^{+}(a,\alpha) + \dot{F}^{+}(a,\alpha) \tag{12a}$$

$$H(\alpha) = ik\beta H_0^{(1)}(Ka) - KH_1^{(1)}(Ka) \tag{12b}$$

Substituting equation (11) into equation (8) yields

$$F^{-}(\rho,\alpha) + F^{+}(\rho,\alpha) = W^{+}(\alpha)\frac{H_0^{1}(K\rho)}{H(\alpha)} \tag{13}$$

In the region $\rho < a$, $z > l$. By taking the half-range Fourier transform of the Helmholtz equation satisfied by $u_2(\rho, z)$, we get

$$\left[\frac{1}{\rho}\frac{\partial}{\partial\rho}\left(\rho\frac{\partial}{\partial\rho}\right) + K^2(\alpha)\right]G^{+}(\rho,\alpha) = f(\rho) - i\alpha g(\rho) \tag{14}$$

where $G^{+}(\rho,\alpha)$ is an analytic function in the upper $\alpha$-plane $\Im m\alpha > \Im m(-k)$, defined by

$$G^{+}(\rho,\alpha) = \int_l^{\infty} u_2(\rho,z)e^{i\alpha(z-l)}\mathrm{d}z \tag{15}$$

while $f(\rho)$ and $g(\rho)$ stand for

$$f(\rho) = \frac{\partial}{\partial z} u_2(\rho, l), \quad \mathrm{g}(\rho) = \mathrm{u}_2(\rho, \mathrm{l}) \tag{16a,b}$$

Particular solution of equation (14) can be found easily by using Green's function which satisfies the Helmholtz equation

$$\left[\frac{1}{\rho}\frac{\partial}{\partial \rho}\left(\rho \frac{\partial}{\partial \rho}\right) + K^2(\alpha)\right]\tilde{G}(\rho, t, \alpha) = 0 \quad \rho \neq t, \quad \rho, t \in (0, a) \tag{17}$$

with the following conditions

$$\begin{aligned} \tilde{G}(0, t, \alpha) &\sim \text{bounded} \\ \tilde{G}(t+0, t, \alpha) - \tilde{G}(t-0, t, \alpha) &= 0 \\ \frac{\partial}{\partial \rho}\tilde{G}(t+0, t, \alpha) - \frac{\partial}{\partial \rho}\tilde{G}(t-0, t, \alpha) &= \frac{1}{t} \\ \left(ik\beta + \frac{\partial}{\partial \rho}\right)\tilde{G}(a, t, \alpha) &= 0 \end{aligned} \tag{18a, b, c, d}$$

The solution is

$$\tilde{G}(\rho, t, \alpha) = \frac{1}{J(\alpha)} Q(\rho, t, \alpha) \tag{19}$$

with

$$Q(\rho, t, \alpha) = \frac{\pi}{2}\begin{cases} J_0(K\rho)[JY_0(Kt) - YJ_0(Kt)] & 0 \leq \rho \leq t \\ J_0(Kt)[JY_0(K\rho) - YJ_0(K\rho)], & t \leq \rho \leq a \end{cases} \tag{20}$$

where

$$J = J(\alpha) = ik\beta J_0(Ka) - KJ_1(Ka) \tag{21a}$$

$$Y = Y(\alpha) = ik\beta Y_0(Ka) - KY_1(Ka) \tag{21b}$$

The solution of equation (14) can now be written as

$$G^+(\rho, \alpha) = \frac{1}{J(\alpha)}\left[B(\alpha)J_0(K\rho) + \int_0^a (f(t) - i\alpha g(t))Q(t, \rho, \alpha)t\mathrm{d}t\right] \tag{22}$$

where $B(\alpha)$ stands for the spectral coefficient to be determined. Using equations (3d) and (3e), substituting equation (22) and its derivative with respect to $\rho$, $B(\alpha)$ can be solved to give

$$B(\alpha) = W^+(\alpha) \tag{23}$$

Inserting now equation (23) into equation (22) we get

$$G^{+}(\rho,\alpha)=\frac{1}{J(\alpha)}\left[W^{+}(\alpha)J_0(K\rho)+\int_0^a (f(t)-i\alpha g(t))Q(t,\rho,\alpha)t\mathrm{d}t\right] \tag{24}$$

The left hand side of equation (24) is analytic in the upper half-plane $\Im m\alpha > \Im m(-k)$. The regularity of the right hand side may be violated by the presence of the simple poles occurring at the zeros of $J(\alpha)$ lying in the upper $\alpha$-half plane, namely at $\alpha=\alpha_m$.

$$ika\beta J_0(\gamma_m)-\gamma_m J_1(\gamma_m)=0 \tag{25a}$$

$$\alpha_m=\sqrt{k^2-\left(\frac{\gamma_m}{a}\right)^2},\quad \Im\mathrm{m}\alpha_\mathrm{m}\geq\Im\mathrm{m}k \tag{25b}$$

In order that the right hand side of equation (24) be also analytic at $\alpha=\alpha_m$, we should have

$$W^{+}(\alpha_m)=\frac{a}{2}J_0(\gamma_m)\left[1-(\beta ka/\gamma_m)^2\right][f_m-i\alpha_m g_m] \tag{26}$$

with

$$\begin{bmatrix}f_m\\ g_m\end{bmatrix}=\frac{2}{a^2J_0^2(\gamma_m)\left[1-(\beta ka/\gamma_m)^2\right]}\int_0^a\begin{bmatrix}f(t)\\ g(t)\end{bmatrix}J_0\left(\frac{\gamma_m}{a}t\right)t\mathrm{d}t \tag{27}$$

By using the continuity relation (3e), it gives

$$G^{+}(a,\alpha)=F^{+}(a,\alpha) \tag{28}$$

and considering equation (13), we obtain

$$\frac{W^{+}(\alpha)}{M(\alpha)}-\frac{a}{2}F^{-}(a,\alpha)=-\frac{1}{2J(\alpha)}\int_0^a (f(t)-i\alpha g(t))J_0(Kt)t\mathrm{d}t \tag{29}$$

where

$$M(\alpha)=\pi iJ(\alpha)H(\alpha) \tag{30}$$

Owing to equation (27), $f(\rho)$ and $g(\rho)$ can be expanded into Dini series as follows

$$f(\rho)=\sum_{m=1}^{\infty}f_m J_0\left(\frac{\gamma_m}{a}\rho\right),\quad g(\rho)=\sum_{m=1}^{\infty}g_m J_0\left(\frac{\gamma_m}{a}\rho\right) \tag{31a,b}$$

Substituting equations (31a) and (31b) in equation (29) and evaluating the resultant integral, one obtains the following modified Wiener–Hopf equation valid in the strip $\Im m(-k) < \Im m\alpha < \Im mk$.

$$\frac{W^+(\alpha)}{M(\alpha)} - \frac{a}{2}F^-(a,\alpha) = \frac{a}{2}\sum_{m=1}^{\infty}\frac{J_0(\gamma_m)}{\alpha_m^2 - \alpha^2}[f_m - i\alpha g_m] \tag{32}$$

## *Solution of the modified Wiener–Hopf equation*

The formal solution of equation (32) can easily be obtained through the classical Wiener–Hopf procedure.[18] The result is

$$\frac{W^+(\alpha)}{M_+(\alpha)} = \frac{a}{2}\sum_{m=1}^{\infty}\frac{J_0(\gamma_m)[f_m + i\alpha_m g_m]M_+(\alpha_m)}{2\alpha_m(\alpha + \alpha_m)} \tag{33}$$

where $M_+(\alpha)$ is the split function, analytic and free of zeros in the upper half-plane $\Im m\alpha > \Im m(-k)$, resulting from the Wiener–Hopf factorization of the functions $M(\alpha)$ as

$$M(\alpha) = M_+(\alpha)M_-(\alpha), \quad M_-(\alpha) = M_+(-\alpha) \tag{34a,b}$$

The explicit expressions of $M_+(\alpha)$ is given in Buyukaksoy and Polat[19] as follows

$$\begin{aligned} M_+(\alpha) = {} & \sqrt{\pi i\left(ik\beta J_0(ka) - kJ_1(ka)\right)}\sqrt{\left(ik\beta H_0^{(1)}(ka) - kH_1^{(1)}(ka)\right)} \\ & \times \exp\left\{i\frac{a\alpha}{\pi}\left[1 - C + \log\left(\frac{2\pi}{ka}\right) + i\frac{\pi}{2}\right] - \frac{ika}{2}\right\} \\ & \times \exp\left(\frac{aK(\alpha)}{\pi}\log\left(\frac{\alpha + iK(\alpha)}{k}\right) + q(\alpha)\right)\prod_{m=1}^{\infty}\left(1 + \frac{\alpha}{\alpha_m}\right)\exp\left(\frac{i\alpha a}{m\pi}\right) \end{aligned} \tag{35}$$

where $C$ is the Euler's constant given by $C = 0{\cdot}57721$ and $q(\alpha)$ stands for

$$q(\alpha) = \frac{1}{\pi}P\int_0^{\infty}\left[1 - \frac{2}{\pi x}\frac{x^2 - (\beta ka)^2}{\mu(x)}\right]\log\left(1 + \frac{\alpha a}{\sqrt{(ka)^2 - x^2}}\right)\mathrm{d}x \tag{36a}$$

$$\mu(x) = (i\beta kaJ_0(x) - xJ_1(x))^2 + (i\beta kaY_0(x) - xY_1(x))^2 \tag{36b}$$

In equation (36a), $P$ denotes the Cauchy principle value at the singularities $x = ka$. Note that, when we let $|\alpha| \to \infty$ in their respective regions of regularity, we have

$$M_\pm(\alpha) = (\pm\alpha^{1/2}) \tag{37}$$

### *Determination of the constants $f_m$, $g_m$ and $c_m$*

Consider now the waveguide region $\rho < a$, $z < l$ where the total field can be expressed in terms of Dini series as follows

$$u_3(\rho, z) = \sum_{n=1}^{\infty} \left[a_n e^{i\chi_n z} + b_n e^{-i\chi_n z}\right] J_0\left(\frac{\xi_n}{a}\rho\right) \tag{38}$$

with

$$ika\eta J_0(\xi_n) + \xi_n J_1(\xi_n) = 0 \tag{39a}$$

$$n = 1, 2, .., \quad \chi_n = \sqrt{k^2 - \left(\frac{\xi_n}{a}\right)^2} \tag{39b}$$

Consider now the continuity relation in equations (3f) and (3g), namely

$$f(\rho) = \frac{\partial}{\partial z} u_2(\rho, l) = \frac{\partial}{\partial z} u_3(\rho, l) \tag{40a}$$

$$g(\rho) = u_2(\rho, l) = u_3(\rho, l) \tag{40b}$$

Inserting the series expansions of $f(\rho)$ and $g(\rho)$ given in equations (31a) and (31b) in equations (40a) and (40b) respectively, and using equation (38), we get

$$\sum_{m=1}^{\infty} f_m J_0\left(\frac{\gamma_m}{a}\rho\right) = i\sum_{n=1}^{\infty} \chi_n \left[a_n e^{i\chi_n l} - b_n e^{-i\chi_n l}\right] J_0\left(\frac{\xi_n}{a}\rho\right) \tag{41a}$$

$$\sum_{m=1}^{\infty} g_m J_0\left(\frac{\gamma_m}{a}\rho\right) = \sum_{n=1}^{\infty} \left[a_n e^{i\chi_n l} + b_n e^{-i\chi_n l}\right] J_0\left(\frac{\xi_n}{a}\rho\right) \tag{41b}$$

Multiplying both sides of equations (41a) and (41b) by $\rho J_0\left(\frac{\xi_l}{a}\rho\right)$ and integrating from 0 to $a$, we obtain

$$a_n = \frac{a^2 e^{-i\chi_n l}}{2i\chi_n P_n} \sum_{m=1}^{\infty} \frac{f_m + i\chi_n g_m}{\xi_n^2 - \gamma_m^2} \; J_0(\gamma_m)\xi_n J_1(\xi_n)\left(1 + \frac{\beta}{\eta}\right) \tag{42a}$$

$$b_n = -\frac{a^2 e^{i\chi_n l}}{2i\chi_n P_n} \sum_{m=1}^{\infty} \frac{f_m - i\chi_n g_m}{\xi_n^2 - \gamma_m^2} \; J_0(\gamma_m)\xi_n J_1(\xi_n)\left(1 + \frac{\beta}{\eta}\right) \tag{42b}$$

where

$$P_n = \frac{a^2}{2}\left[J_0^2(\xi_n) + J_1^2(\xi_n)\right] \tag{42c}$$

In region $\rho < a$, $z < 0$, $u_4(\rho, z)$ can be expressed as

$$u_4(\rho, z) = \sum_{n=0}^{\infty} c_n e^{-i\sigma_n z} J_0\left(\frac{j_n}{a}\rho\right) \tag{43a}$$

with

$$J_1(j_n) = 0, \quad \sigma_n = \sqrt{k^2 - \left(\frac{j_n}{a}\right)^2}, \quad \sigma_0 = k \tag{43b}$$

from the continuity relations which is given in equations (3h) and (3i) we write

$$\sum_{n=1}^{\infty} [a_n + b_n] J_0\left(\frac{\xi_n}{a}\rho\right) = \sum_{m=0}^{\infty} c_m J_0\left(\frac{j_m}{a}\rho\right) + 1 \tag{44a}$$

$$i\sum_{n=1}^{\infty} \chi_n [a_n - b_n] J_0\left(\frac{\xi_n}{a}\rho\right) = -i\sum_{m=0}^{\infty} \sigma_m c_m J_0\left(\frac{j_m}{a}\rho\right) + ik \tag{44b}$$

after simple operations, one can write

$$a_n = \frac{a^2}{2\chi_n P_n}\left\{\sum_{m=0}^{\infty} c_m \frac{\xi_n J_0(j_m) J_1(\xi_n)}{\xi_n^2 - j_m^2}(\chi_n - \sigma_m) + \frac{J_1(\xi_n)}{\xi_n}(\chi_n + k)\right\} \tag{45a}$$

and

$$b_n = \frac{a^2}{2\chi_n P_n}\left\{\sum_{m=0}^{\infty} c_m \frac{\xi_n J_0(j_m) J_1(\xi_n)}{\xi_n^2 - j_m^2}(\chi_n + \sigma_m) + \frac{J_1(\xi_n)}{\xi_n}(\chi_n - k)\right\} \tag{45b}$$

consider equations (45a) and (45b) together with equations (42a) and (45b), namely

$$\sum_{m=1}^{\infty} \frac{f_m + i\chi_n g_m}{\xi_n^2 - \gamma_m^2} J_0(\gamma_m) = \frac{\eta}{\beta + \eta} i e^{i\chi_n l} \sum_{m=0}^{\infty} c_m \frac{J_0(j_m)}{\xi_n^2 - j_m^2}(\chi_n - \sigma_m) + \frac{\eta}{\beta + \eta} i e^{i\chi_n l} \frac{\chi_n + k}{\xi_n^2} \tag{46a}$$

$$\sum_{m=1}^{\infty} \frac{f_m - i\chi_n g_m}{\xi_n^2 - \gamma_m^2} J_0(\gamma_m) = -\frac{\eta}{\beta + \eta} i e^{-i\chi_n l} \sum_{m=0}^{\infty} c_m \frac{J_0(j_m)}{\xi_n^2 - j_m^2}(\chi_n + \sigma_m) - \frac{\eta}{\beta + \eta} i e^{-i\chi_n l} \frac{\chi_n - k}{\xi_n^2} \tag{46b}$$

By substituting $\alpha = \alpha_1, \alpha_2, \alpha_3, \ldots$ in equation (33) and using equation (26), one can obtain

$$\frac{J_0(\gamma_r)\left[1 - (\beta k a/\gamma_r)^2\right][f_r - i\alpha_r g_r]}{M_+(\alpha_r)} = \sum_{m=1}^{\infty} \frac{J_0(\gamma_m)[f_m + i\alpha_m g_m] M_+(\alpha_m)}{2\alpha_m(\alpha_r + \alpha_m)} \tag{46c}$$

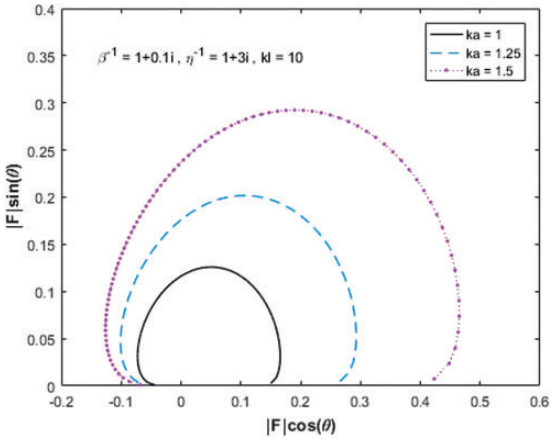


**Figure 3.** Polar plot of the far field amplitude function $\mathcal{F}(\theta)$ versus pipe radius.

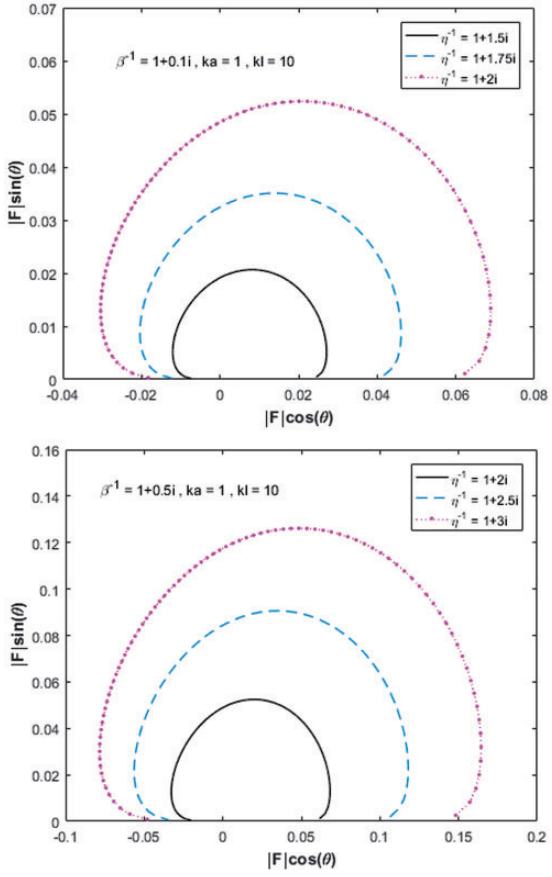


**Figure 4.** Polar plot of the far field amplitude function $\mathcal{F}(\theta)$ versus $\mathrm{Im}\eta^{-1}$ (reactance).

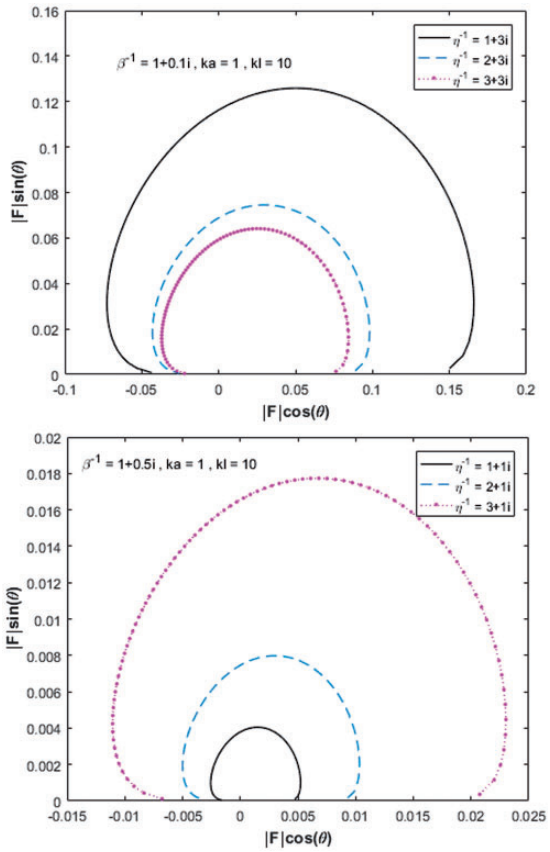


**Figure 5.** Polar plot of the far field amplitude function $\mathcal{F}(\theta)$ versus $\mathrm{Re}\eta^{-1}$ (resistance).

Equations (46a), (46b) and (46c) are the required linear systems of algebraic equations which permits us to determine $f_m$, $g_m$ and $c_m$.

## Analysis of the radiated field

The radiated field in the region $\rho > a$ can be obtained by taking the inverse Fourier transform of $F(\rho, \alpha)$. By using (11), we write

$$u_1(\rho, z) = \frac{1}{2\pi} \int_{\mathcal{L}} W^+(\alpha) \frac{H_0^{(1)}(K\rho)}{H(\alpha)} e^{-i\alpha(z-l)} d\alpha \tag{47}$$

where $\mathcal{L}$ is a straight line parallel to the real $\alpha$-axis, lying in the strip $\Im m(-k) < \Im m\alpha < \Im mk$. Utilizing the asymptotic expansion of $H_0^{(1)}(K\rho)$ as $k\rho \to \infty$

$$H_0^{(1)}(K\rho) = \sqrt{\frac{2}{\pi K\rho}} e^{iK\rho - i\pi/4} \tag{48}$$

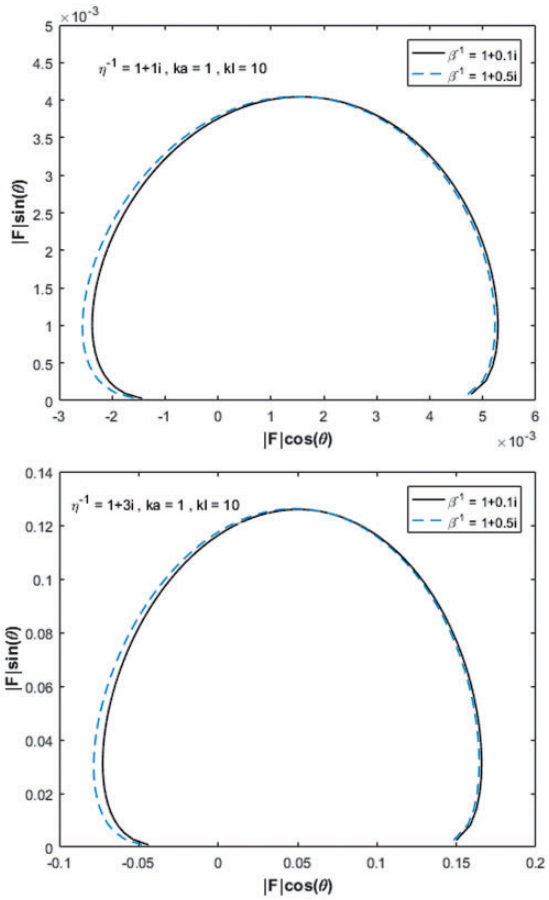


**Figure 6.** Polar plot of the far field amplitude function $\mathcal{F}(\theta)$ versus $\mathrm{Im}\beta^{-1}$ (reactance).

Equation (47) can be evaluated through the saddle-point technique to give

$$u_1(\rho, z) \sim \mathcal{F}(\theta)\frac{e^{ikr}}{kr} \tag{49a}$$

where

$$\mathcal{F}(\theta) = \frac{k}{i\pi}\frac{W^+(-k\cos\theta)}{H(-k\cos\theta)} \tag{49b}$$

where $r$ and $\theta$ are the spherical coordinates defined by

$$\rho = r\sin\theta, \quad z - l = r\cos\theta \tag{50a,b}$$

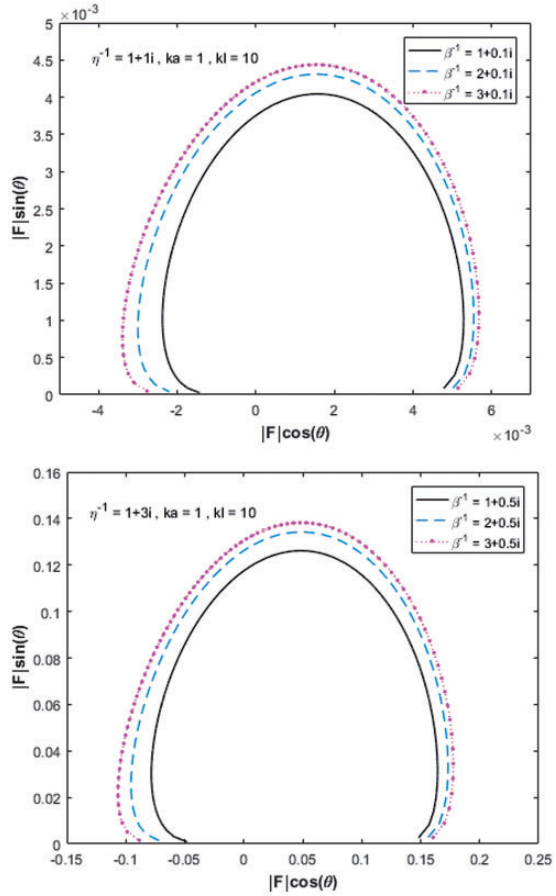


**Figure 7.** Polar plot of the far field amplitude function $\mathcal{F}(\theta)$ versus $\mathrm{Re}\beta^{-1}$ (resistance).

## Graphics

This section presents some graphics to illustrate the effects of geometrical and physical parameters like surface impedances, pipe radius and extension etc. All the numerical results are derived by truncating the infinite series and the infinite systems of linear algebraic equations after the first $N$ terms. It is seen that the amplitude of the radiated field becomes insensitive to the increase of the truncation number after $N = 20$.

In Figure 3, one can see that, the amplitude of the radiated field increases with increasing values of $ka$. Figures 4 to 7 shows the variation of the amplitude of the radiated field for the values of reactance and resistance. As it can be seen that, the radiated field can be reduced by changing the values of $\mathrm{Im}\beta^{-1}$, $\mathrm{Im}\eta^{-1}$ and $\mathrm{Re}\beta^{-1}$, $\mathrm{Re}\eta^{-1}$. From Figures 8 to 10, in all far field graphs, some amount of decrease in the radiated field in all directions is observed in comparison with the hard ($\beta \to 0$, $\eta \to 0$ or $\beta, \eta \to 0$) walled duct. In Figure 11, the radiated field amplitude decreases with increasing value of $kl$. Figure 12 displays the variation of the modulus of the reflection coefficient $|c_0|$ with respect to the wave number $k$ for different

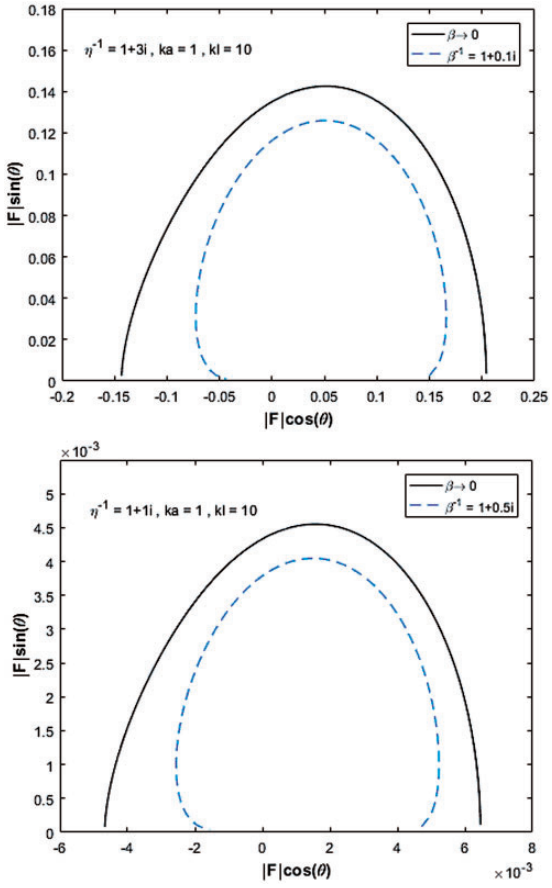


**Figure 8.** Polar plot of the far field amplitude function $\mathcal{F}(\theta)$ versus rigid-lined outer surface.

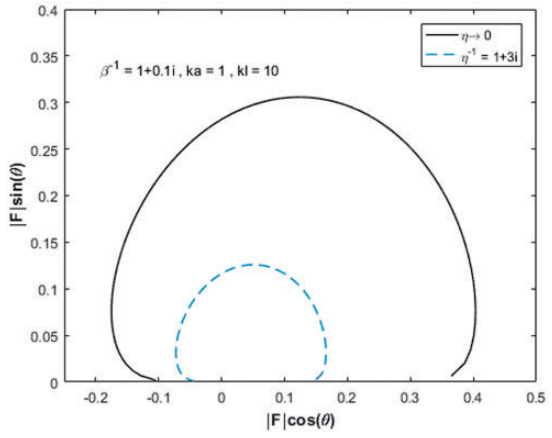


**Figure 9.** Polar plot of the far field amplitude function $\mathcal{F}(\theta)$ versus rigid-lined inner surface.

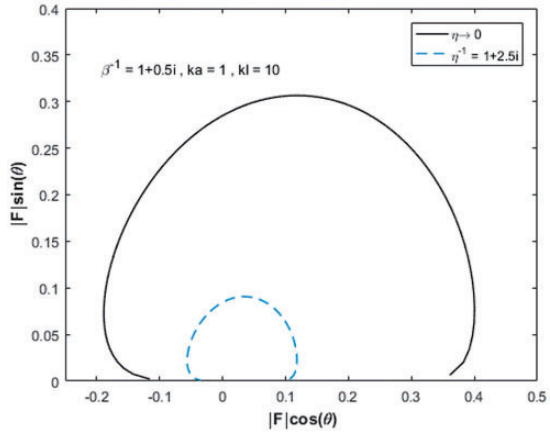


**Figure 9.** Continued

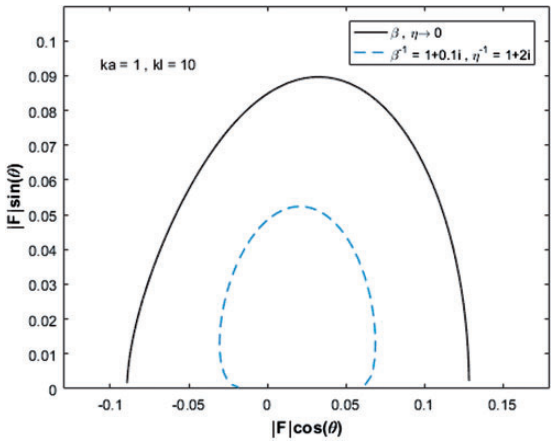


**Figure 10.** Polar plot of the far field amplitude function $\mathcal{F}(\theta)$ versus rigid-lined pipe.

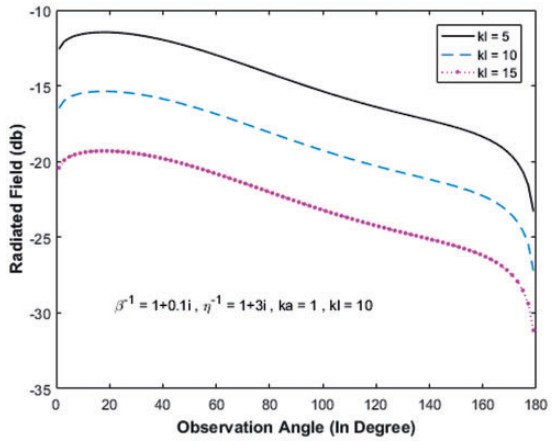


**Figure 11.** $20log(\mathcal{F}(\theta))$ versus the observation angle for different pipe extension.

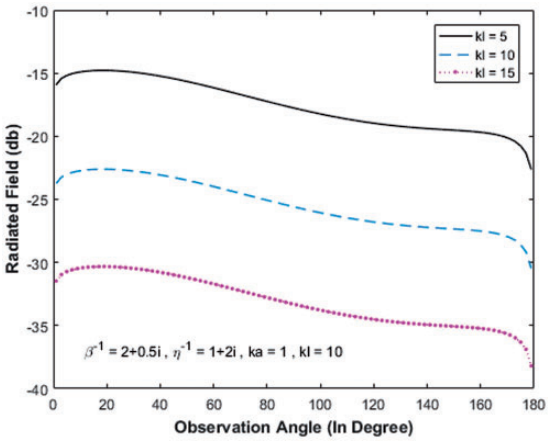


**Figure 11.** Continued

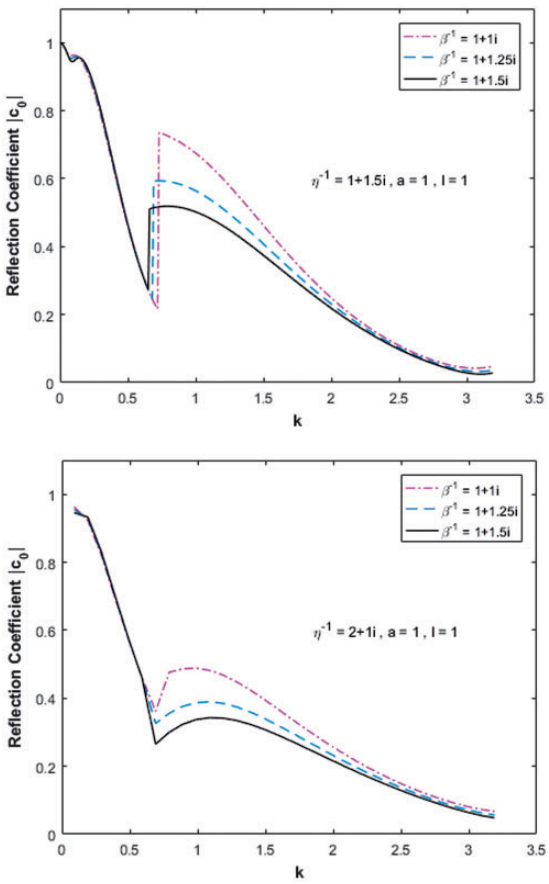


**Figure 12.** Variation of reflection coefficient $|c_0|$ versus the wave number k for different values of outer surface impedance.

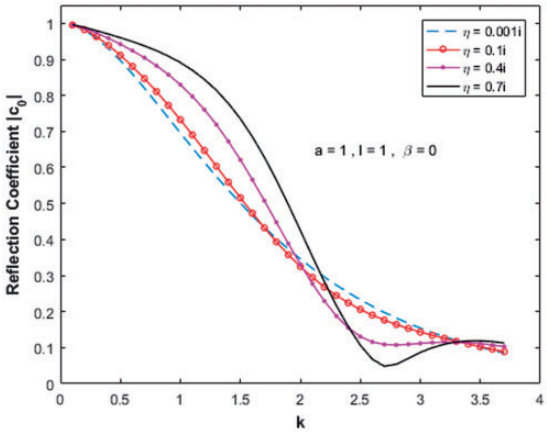


**Figure 13.** Comparison of the reflection coefficient $|c_0|$ with the study of Demir and Buyukaksoy.[17]

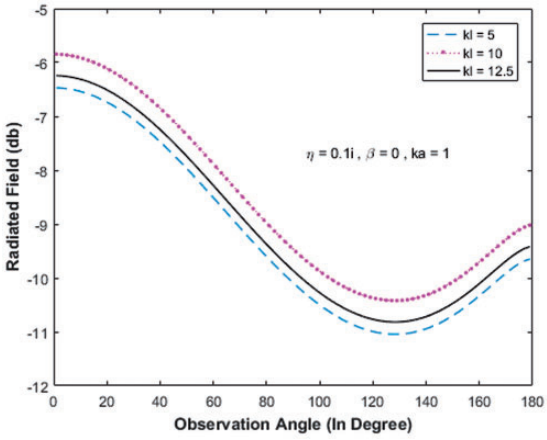


**Figure 14.** Comparison of the radiated field with the study of Demir and Buyukaksoy.[17]

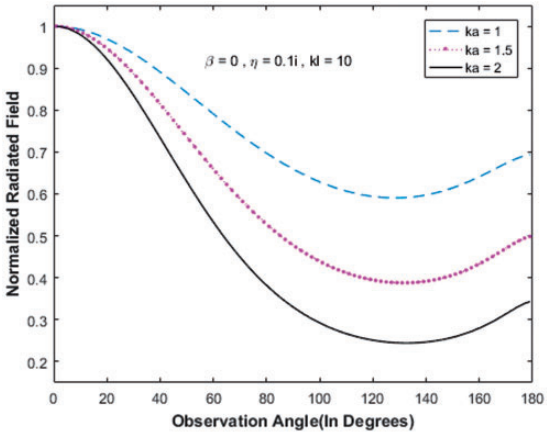


**Figure 15.** Comparison of the normalized radiated field with the study of Demir and Buyukaksoy.[17]

values of the outer lining. From the graphs of the reflection coefficient, it can be seen that the magnitude $|c_0|$ falls off as $k$ increases. Beyond this frequency the magnitude again increases, but not to the high values achieved in the principal frequency range.

Finally, Figures 13 to 15 display an excellent agreement, in both the reflection coefficient $|c_0|$ and the radiated field, between the present paper and the previous study.[17]

## Conclusions

This study is carried out to obtain the radiation characteristics from a semi-infinite coated pipe with partial internal lining. By means of the Fourier transform technique in conjunction with the Mode Matching method, the boundary value problem is reduced to modified Wiener–Hopf equation of the second kind whose solution is obtained by performing the Wiener–Hopf factorization and decomposition procedures. The final solution involves three systems of linear algebraic equations involving three sets of infinitely many unknown coefficients. Numerical solution to these systems is obtained for various values of the problem parameters such as pipe radius, internal and external surface impedances, pipe extension, etc. It can be easily checked that for $\beta = 0$, perfect agreement is observed with the study of Demir and Buyukaksoy[17] both analytically and numerically. Furthermore, it is observed that choosing impedance values appropriately, it is possible to attenuate radiation.

### Acknowledgements

The first author would like to thank TUBITAK (The Scientific and Technological Research Council of Turkey) for continued support.

### Declaration of conflicting interests

The author(s) declared no potential conflicts of interest with respect to the research, authorship, and/or publication of this article.

### Funding

The author(s) received no financial support for the research, authorship, and/or publication of this article.

### References

1. Stansfeld SA and Matheson MP. Noise pollution: non-auditory effects on health. *Br Med Bull* 2003; 68: 243–257.
2. Ising H and Kruppa B. Health effects caused by noise: evidence in the literature from the past 25 years. *Noise Health* 2004; 22: 5–13.
3. Fiedler PEK and Zannin PHT. Evaluation of noise pollution in urban traffic hubs – noise maps and measurements. *Environ Impact Assess* 2015; 51: 1–9.
4. Recio A, Linares C, Banegas JR, et al. Road traffic noise effects on cardio vascular, respiratory, and metabolic health: an integrative model of biological mechanisms. *Environ Res* 2016; 146: 359–370.
5. Buyukaksoy A and Demir A. Radiation of sound from a semi-infinite rigid duct inserted axially into a larger innite tube with wall impedance discontinuity. *Z Angew Math Mech* 2006; 86: 563–571.
6. Demir A and Rienstra SW. Sound radiation from a lined exhaust duct with lined afterbody. In: *16th AIAA/CEAS aeroacoustics conference*. Reston: AIAA, 2010, pp. 1–18.

7. Choi W, Woodhouse J and Langley RS. *Sound radiation from a vibrating plate with uncertainty*. *J Sound Vib* 2004; 333: 3966–3980.
8. Campos LMBC and Oliveira JMGS. On sound radiation from an open-ended non-uniformly lined cylindrical nozzle. *Acta Acust United Acust* 2014; 100: 795–809.
9. Lindberg A and Pavic G. Computation of sound radiation by a driver in a cabinet using a substitute source approach. *J Acoust Soc Am* 2015; 138: 1132–1144.
10. Zhang X, Squicciarini G and Thompson DJ. Sound radiation of a railway rail in close proximity to the ground. *J Sound Vib* 2016; 362: 111–124.
11. Hassan M and Rawlins AD. Sound radiation in a planar trifurcated lined duct. *Wave Motion* 1999; 29: 157–174.
12. Rienstra SW. Acoustic scattering at a hard-soft lining transition in a flow duct. *J Eng Math* 2007; 59: 451–475.
13. Auregan Y and Pagneux V. Slow sound in lined flow ducts. *J Acoust Soc Am* 2015; 138: 6051–6019.
14. Demir A. Scattering matrices in non-uniformly lined ducts. *Z Angew Math Phys* 2017; 68: 1–15.
15. Rawlins AD. Radiation of sound from an unanged rigid cylindrical duct with an acoustically absorbing internal surface. *Z Proc Roy Soc Lond* 1978; 361: 65–91.
16. Noble B. *Methods based on the Wiener–Hopf technique*. 2nd ed. New York: Chelsea Publishing Company, 1988.
17. Demir A and Buyukaksoy A. *Radiation of plane sound waves by a rigid circular cylindrical pipe with a partial internal impedance loading*. *Acta Acust United Acust* 2003; 89: 578–585.
18. Mittra R and Lee SW. *Analytical techniques in the theory of guided waves*. New York: McMillan, 1971.
19. Buyukaksoy A and Polat B. *Diffraction of acoustic waves by a semi-infinite cylindrical impedance pipe of certain wall thickness*. *J Eng Math* 1998; 33: 333–352.